Prediction of Heat-Affected Zone Characteristics in Submerged Arc Welding of Structural Steel Pipes

Mathematical models were developed to study the effects of process variables and heat input on the HAZ of submerged arc welds in structural steel pipes

BY V. GUNARAJ AND N. MURUGAN

ABSTRACT. In submerged arc welding (SAW), selecting appropriate values for process variables is essential in order to control heat-affected zone (HAZ) dimensions and get the required bead size and quality. Also, conditions must be selected that will ensure a predictable and reproducible weld bead, which is critical for obtaining high quality. In this investigation, mathematical models were developed to study the effects of process variables and heat input on various metallurgical aspects, namely, the widths of the HAZ, weld interface, and grain growth and grain refinement regions of the HAZ. The color metallography technique and response surface methodology were also used. Direct and interaction effects of the process variables and heat input on the characteristics of the HAZ were presented in graphical forms. The study revealed: 1) heat input and wire feed rate have a positive effect, but welding speed has a negative effect on all HAZ characteristics; 2) width of grain growth and grain refinement zones increased and weld interface decreased with an increase in arc voltage; and 3) width of HAZ is maximum (about 2.2 mm) when wire-feed rate and welding speed are at their minimum limits.

Introduction

In any welding process, the microstructure of the weldment undergoes considerable changes because of the heating and cooling cycle of the weld zone, which in turn is directly related to the welding process and techniques employed. Only by improving the microstructure of the HAZ can the properties of a welded joint be improved. In general, a number of welding process variables and operating conditions influence the characteristics and microstructure, and, therefore, hardness, toughness, and cracking susceptibility of the HAZ in steel fusion welds (Ref. 1). Excessive heat input could result in a wide HAZ with low impact strength, particularly in high-heat-input submerged arc welds.

From a metallurgical point of view, the heat-affected zone of a fusion weld in steel may be divided into three zones (Ref. 2), supercritical, intercritical, and subcritical, as shown in Fig. 1A. The supercritical region may, in turn, be divided into two regions — grain growth and grain refinement — as shown in Fig. 1B. The microstructure of the grain growth and grain refinement regions of the HAZ's supercritical zone influence the properties of the weld joint. To predict the properties of this zone, one must know the amount and extent of grain growth and the weld thermal cycle. Heat input from the welding process must be limited so as to keep the width of the HAZ's supercritical zone as narrow as possible. Also, the supercritical zone undergoes considerable microstructural changes that compare to small, negligible, structural changes in the HAZ's intercritical and subcritical zones. These microstructural changes affect the mechanical and metallurgical properties of the weldment (Ref. 3). Therefore, the size of the HAZ is an indication of the extent of structural changes. Because HAZ dimensions are controlled by process variables and heat input, they have to be correlated through development of mathematical models.

With a view to achieving the abovementioned aim, statistically designed experiments based on the factorial technique were used to reduce cost and time, as well as to obtain the required information about the main and interaction effects of process variables on response parameters (Refs. 4, 5). The mathematical models thus developed are useful for selecting correct process variables for achieving the desired weld bead HAZ characteristics and mechanical properties and to predict HAZ dimensions for the given process variables (Ref. 6). They also help to improve understanding of the effect of process parameters on bead quality, for quantitative evaluation of the interaction effects of process variables on HAZ characteristics, and to optimize the size of the weld bead's HAZ inorder to obtain a better quality welded joint with desirable properties at a relatively low cost.

KEY WORDS

Heat-Affected Zone
Weld Interface
Supercritical Zone
Grain Growth Zone
Grain Refinement Zone
Heat Input
Microstructure
Regression Analysis
ANOVA Technique
and Responses

Experimental Procedure

The experiment was conducted at M/s. Sri Venkateswara Engineering Corp., Coimbatore, India, with the following setup.

ADORE semiautomatic welding equipment with a 1200-A-capacity, constant voltage, rectifier-type power source was used to weld 300 x 150 x 6-mm IS: 2062 structural steel plates. ESAB SA1

V. GUNARAJ is Assistant Professor of Mechanical Engineering, Kumaraguru College of Technology, Coimbatore, Tamil Nadu, India. N. MURUGAN is Assistant Professor of Mechanical Engineering, Coimbatore Institute of Technology, Coimbatore, Tamil Nadu, India.

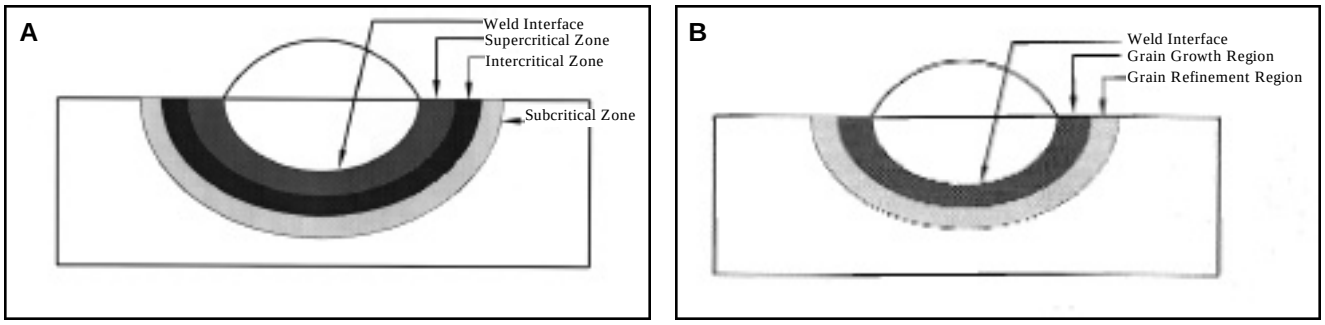

Fig. 1 — A — The different areas of the heat-affected zone; B — the different regions of the supercritical zone of the heat-affected zone.

(E 8), 3.15-mm-diameter, copper-coated electrode in coil form and ESAB basic fluoride-type (equivalent to DIN 8557) granular flux were used. A weld bead was laid on the plate surface.

Investigation Plan

The research was carried out using the following steps (Ref. 7):

1) Identifying the important process control variables and finding their upper and lower limits;
2) Developing the design matrix;
3) Conducting the experiments as per the design matrix;
4) Recording the responses;
5) Developing the mathematical models;
6) Calculating the coefficients of the polynomials;
7) Checking the adequacy of the models developed;
8) Calculating the significance of the coefficients and arriving at final mathematical models;
9) Conducting the conformity test;
10) Determining the quantitative effects of process variables and heat input on weld bead HAZ.

Identification of the Process Variables and Finding Their Limits

The independently controllable process parameters affecting bead geometry and weld bead quality were arc voltage (V), wire feed rate (F), welding speed (S), and nozzle-to-plate distance (N). Trial runs were carried out by varying one of the process parameters while keeping the rest at constant values (Ref. 8). The working range was decided upon by inspecting the bead for a smooth appearance without any visible defects such as surface porosity and undercut. The upper limit of a factor was coded as +2 and the lower limit as –2. The coded values for intermediate values were calculated from the following relationship: $X_i = 2[2X - (X_{max} + X_{min})]/(X_{max} - X_{min})$, where X_i is the required coded value of a variable X; X is any value of the variable from X_{min} to X_{max}; X_{min} is the lower level of the variable; and X_{max} is the upper level. The process variables with their units and notations are given in Table 1.

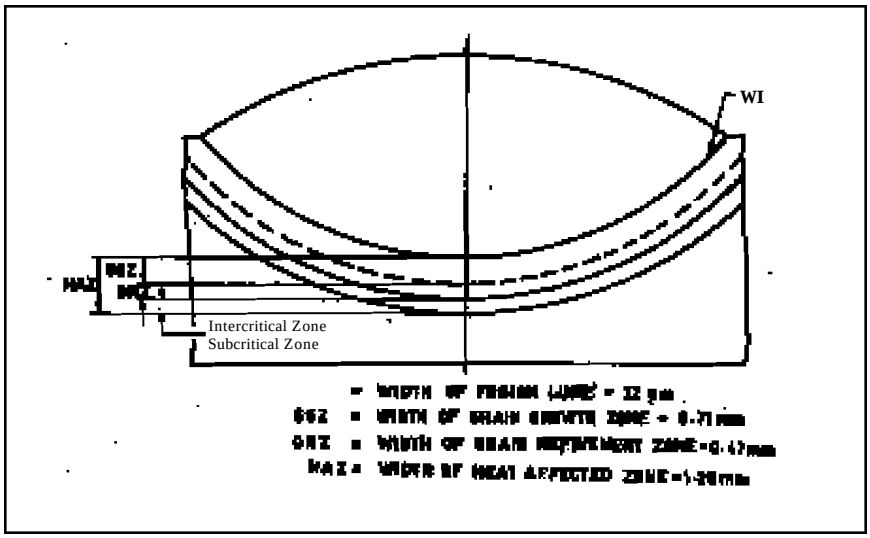

Fig. 2 — Cross section of a typical welded speciment (specimen No. 2, 10X). WI = width of the weld interface = 32 μm, GGZ = width of grain growth zone = 0.71 μm; GRZ = width of grain refinement zone = 0.47 μm; HAZ = width of heat-affected zone = 1.28.

Table 1 — Process Control Parameters and Their Limits

Parameters	Units	Notation	Limits –2	–1	0	+1	+2
Arc voltage	volts	V	24	26	28	30	32
Wire feed rate	m/min	F	0.70	0.93	1.16	1.39	1.62
Welding speed	m/min	S	0.43	0.51	0.59	0.67	0.75
Nozzle-to-plate distance	mm	N	30.00	32.50	35.0	37.5	40.0

Developing the Design Matrix

The selected design matrix, shown in Table 2, is a five-level, four-factor, central composite rotatable factorial design (Ref. 9) consisting of 31 sets of coded conditions. It comprises a full replication of 2^4 (=16) factorial design plus seven center points and eight star points. All welding variables at their intermediate level (0) constitute the center points and the combinations of each of the welding variables at either its lowest (–2) or highest (+2), with the other three variables at their intermediate level, constitute the star points. Thus, the 31 experimental runs allowed estimation of the linear, quadratic, and two-way interactive effects of the welding variables on the bead geometry.

Conducting the Experiments as Per the Design Matrix

The experiments were conducted as per the design matrix at random to avoid systematic errors infiltrating the system. Weld beads were deposited on the surface of the 6-mm-thick structural steel plates with the experimental setup explained previously.

Recording the Responses

The welded plates were cut at the center of the bead to obtain 10-mm-wide test specimens. The standard metallographic technique, i.e., metal polishing with a series of emery sheets and disc polishing using diamond paste with particle sizes ranging from 5μ to 0.5 μ, was carried out. The established color etching procedure for steel was employed to identify different regions of the weldment. An optical research microscope (NEOPHOT-32) was used. With the help of built-in linear measuring devices in the microscope that had an accuracy of 0.001 mm, dimensions (width) of the weld interface and different regions of the HAZ were measured. These were the width of the heat-affected zone (widths of supercritical zone + intercritical zone + subcritical zone) and the width of the weld interface (WI). The observed and calculated values are given in Table 2. A cross section of a typical welded specimen (Specimen No. 2) is shown in Fig. 2.

Development of Mathematical Models

The response function representing any of the HAZ dimensions can be expressed as y = f (V, F, S, N). The relationship selected, being a second-degree response surface, is expressed as follows (Ref. 10):

$$Y = b_0 + b_1V + b_2F + b_3S + b_4N + b_{11}V^2 + b_{22}F^2 + b_{33}S^2 + b_{44}N^2 + b_{12}VF + b_{13}VS + b_{14}VN + b_{23}FS + b_{24}FN + b_{34}SN \quad 1)$$

Evaluation of the Coefficients of Models

Regression analysis, with the help of the following equations, was used to calculate the values of the coefficients (Ref. 11):

$$b_0 = 0.142857\,\Sigma Y - 0.035714\,\Sigma\Sigma(X_{ii}Y)$$
$$b_i = 0.041667\,\Sigma(X_iY)$$
$$b_{ii} = 0.03125\,\Sigma(X_{ii}Y) - 0.035714\,\Sigma\Sigma\,(X_{ii}Y) - 0.035714\,\Sigma Y$$
$$b_{ij} = 0.0625\,\Sigma(X_{ij}Y)$$

A computer program was used to calculate the values of these coefficients for different responses. The calculated values are presented in Table 3.

Checking the Adequacy of the Developed Models

The adequacy of the models was then tested by the analysis-of-variance technique (ANOVA) (Ref. 11). As per this technique: 1) If the calculated value of the model's F– ratio does not exceed its tabulated value for a desired level of confidence (say 95%); and 2) if the calculated value of the model's R– ratio exceeds its standard tabulated value for a desired level of confidence (again 95%), then the models are adequate (Refs. 11, 12). From Table 4, it is evident that for all models, the above conditions were satisfied and, hence, adequate.

Table 2 — Design Matrix and Observed Values of the HAZ

	Design Matrix				Weld Bead Parameters				
Sl. No.	V	F	S	N	Heat input (HI) kJ/cm	Width of heat-affected zone (HAZ), mm	Width of Weld Interface (WI), μm	Width of grain growth zone (GGZ) mm	Width of grain refinement zone (GRZ), mm
1	–1	–1	–1	–1	9.1	1.31	30	0.69	0.44
2	+1	–1	–1	–1	11.6	1.28	32	0.71	0.47
3	–1	+1	–1	–1	11.6	1.62	40	0.84	0.57
4	+1	+1	–1	–1	14.7	1.55	38	0.82	0.55
5	–1	–1	+1	–1	6.7	1.05	22	0.55	0.27
6	+1	–1	+1	–1	7.4	1.12	24	0.58	0.29
7	–1	+1	+1	–1	8.6	1.18	28	0.66	0.32
8	+1	+1	+1	–1	10.1	1.15	31	0.69	0.38
9	–1	–1	–1	+1	8.7	1.14	29	0.67	0.36
10	+1	–1	–1	+1	11.0	1.12	32	0.65	0.34
11	–1	+1	–1	+1	12.1	1.37	44	0.75	0.46
12	+1	+1	–1	+1	15.0	1.67	56	0.96	0.51
13	–1	–1	+1	+1	6.4	0.91	21	0.43	0.23
14	+1	–1	+1	+1	7.4	0.87	23	0.44	0.21
15	–1	+1	+1	+1	8.2	1.00	25	0.51	0.27
16	+1	+1	+1	+1	10.1	1.21	26	0.64	0.35
17	–2	0	0	0	7.8	1.15	24	0.54	0.27
18	+2	0	0	0	11.8	1.13	25	0.57	0.26
19	0	–2	0	0	7.0	0.92	22	0.47	0.25
20	0	+2	0	0	10.6	1.61	39	0.77	0.58
21	0	0	–2	0	14.2	1.66	47	0.81	0.64
22	0	0	+2	0	7.3	0.98	22	0.53	0.24
23	0	0	0	–2	10.2	1.02	29	0.52	0.28
24	0	0	0	+2	9.5	0.97	26	0.50	0.27
25	0	0	0	0	9.8	1.01	25	0.58	0.29
26	0	0	0	0	9.7	0.98	24	0.57	0.24
27	0	0	0	0	9.7	0.95	26	0.55	0.25
28	0	0	0	0	10.1	1.07	27	0.61	0.29
29	0	0	0	0	9.7	1.02	27	0.59	0.26
30	0	0	0	0	9.8	1.04	25	0.62	0.29
31	0	0	0	0	10.2	1.15	31	0.68	0.31

For each experimental run, arc voltage and arc current were noted. The corresponding heat input was calculated by using the formula

$$\text{Heat input, kJ/cm} = \frac{\text{Arc voltage (volts) x Arc current (amperes)}}{\text{Welding speed (cm/s) x 1000}} \text{ x Arc Efficiency}$$

Arc Efficiency for SAW is taken as 1.

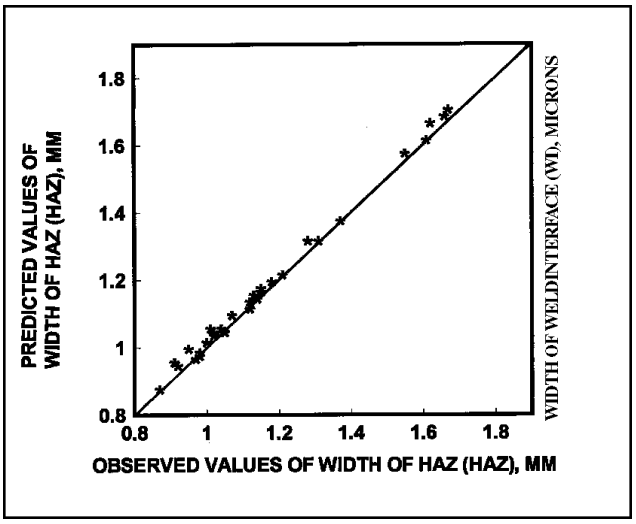

Fig. 3 — Scatter diagram for heat-affected zone width.

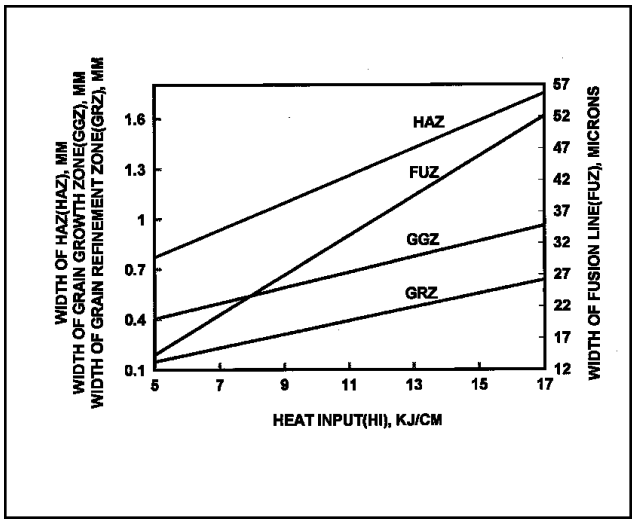

Fig. 4 — Direct effect of heat input on the width of the different HAZ regions.

Testing the Significance of the Coefficients and Development of Final Mathematical Models

The final mathematical models follow. The process control variables are in their coded form. Significance of the coefficients was tested using the SYSTAT software package (Ref. 13). The software's step backward option was used to eliminate insignificant coefficients and to recalculate the values of significant coefficients. Reduced models with significant coefficients were developed. It was found the reduced models were better than the full models because they have higher values of R^2 (adjusted) and lesser values of standard error estimates. The R^2 values and standard error of estimates for both models are given in Table 5. The final reduced mathematical models with the significant coefficients follow:

$$\text{Heat Input, KJ/cm} = 9.78 + 0.996\,V + 1.22\,F - 1.78\,S - 0.244\,F^2 + 0.244\,S^2 + 0.18\,V\,F - 0.356\,V\,S - 0.244\,F\,S \quad (2)$$

$$\text{Width of Heat-Affected Zone, mm} = 1.029 + 0.013\,V + 0.144\,F - 0.159\,S - 0.05\,N + 0.032V^2 + 0.064\,F^2 + 0.078\,S^2 + 0.03\,V\,F + 0.029\,V\,N - 0.056\,F\,S + 0.037\,F\,N \quad (3)$$

$$\text{Width of Weld Interface, } \mu\text{m} = 26.94 + 0.924\,V + 4.529\,F - 6.305\,S + 0.221N^* + 1.431\,F^2 + 2.431\,S^2 - 2.169\,FS + 1.044\,F\,N - 1.956\,S\,N \quad (4)$$

$$\text{Width of Grain Growth Zone, mm} = 0.591 + 0.017\,V + 0.073\,F - 0.089\,S - 0.023\,N + 0.018\,F^2 + 0.031\,S^2 + 0.02\,FS - 0.026\,SN \quad (5)$$

$$\text{Width of Grain Refinement Zone, mm} = 0.282 + 0.061\,F - 0.091\,S - 0.024\,N + 0.039\,F^2 + 0.045\,S^2 \quad (6)$$

Table 3 – Regression Coefficients of Models

Sl. No.	Coefficient	Bead Parameters: Heat Input	Width of HAZ	Width of WI	Width of GGZ	Width of GRZ
1	b_0	9.843	1.032	26.42	0.597	0.275
2	b_1	0.996	0.013	0.924	0.170	0.007
3	b_2	1.220	0.144	4.529	0.073	0.061
4	b_3	–1.780	–0.159	–6.305	–0.089	–0.091
5	b_4	–0.996	–0.050	0.221	–0.023	–0.024
6	b_{11}	0.009	0.033	–0.082	0.003	0.002
7	b_{22}	–0.241	0.064	1.498	0.017	0.039
8	b_{33}	0.247	0.078	2.498	0.030	0.046
9	b_{44}	0.002	–0.003	0.748	–0.010	0.004
10	b_{12}	0.181	0.030	0.489	0.002	0.009
11	b_{13}	–0.356	0.005	–0.261	0.003	0.006
12	b_{14}	0.019	0.029	0.636	0.014	0.001
13	b_{23}	–0.244	–0.056	–2.169	0.020	–0.010
14	b_{24}	0.106	0.037	1.044	0.013	0.007
15	b_{34}	–0.031	0.004	–1.956	–0.026	0.010

Conducting the Conformity Test

Validity of the developed models was further tested by drawing scatter diagrams that show the observed and predicted values of weld bead dimensions. A representative scatter diagram is shown in Fig. 3. To determine accuracy of the models, conformity test runs were conducted. For these runs, process variables were assigned some intermediate values. Responses were measured and presented in Table 6. A comparison was made between actual and predicted values (Table 6). The results show the models' accuracy was above 97%.

Results and Discussions

Effects of process variables on HAZ parameters are shown in Figs. 4–14. These results were used to predict values of the process variables and weld bead HAZ geometry for any given set of process variables for SAW of 6-mm structural steel plates without preheating. Also, values of the control variables and heat input can be obtained for any desirable HAZ parameter value.

Table 4 — Calculation of Variance for Testing the Adequacy of the Models

Bead parameters	First-order terms SS	DF	Second-order terms SS	DF	Lack of fit SS	DF	Error terms SS	DF	F ratio	R ratio	Whether model is adequate
Heat input	138.7	4	7.52	10	1.740	10	0.334	6	3.122	183.7	Adequate
Width of HAZ	1.172	4	0.366	10	0.079	10	0.026	6	1.850	5.00	Adequate
Width of weld interface	1472	4	374.8	10	136.1	10	31.72	6	2.570	24.96	Adequate
Width of grain growth zone	0.34	4	0.063	10	0.051	10	0.011	6	2.800	16.02	Adequate
Width of grain refinement zone	0.30	4	0.100	10	0.021	10	0.004	6	3.110	43.60	Adequate

$R\ ratio_{(14,\,6,\,0.05)}$ = 3.96 = (Sum of squares of first- and second-order terms/Sum of DF of first- and second-order terms)/MS of error terms
$F\ ratio_{(10,\,6,\,0.05)}$ = 4.09 = MS of Lack of fit/MS of error terms.
SS = Sum of squares; DF = Degree of freedom; MS = Mean square = SS/DF

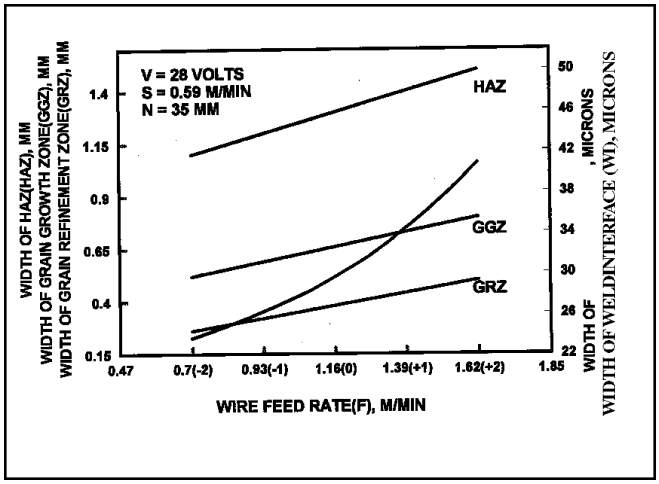

Fig. 5 — Direct effect of wire feed rate on HAZ characteristics.

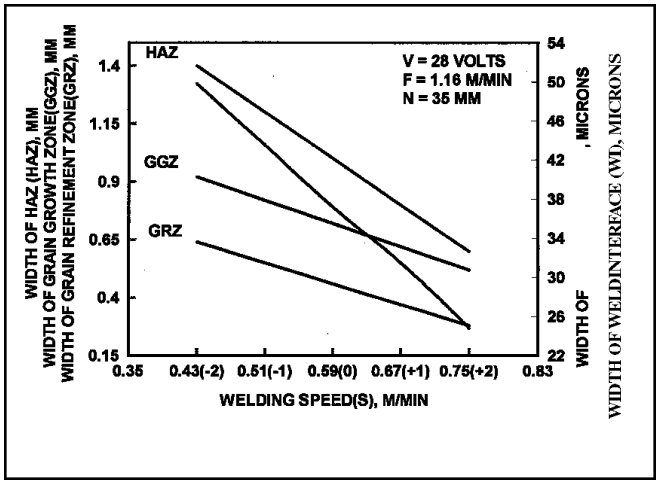

Fig. 6 — Direct effect of welding speed on the width of the different HAZ regions.

Effects of Heat Input

Figure 4 shows the effect of heat input on various dimensions, namely, the widths of the weld interface (WI), grain growth zone (GGZ) and grain refinement zone (GRZ) of the HAZ's supercritical zone, and of the HAZ. From the figure, it is observed these widths all increase with an increase in heat input or arc energy. This is because an increase in heat input results in a decrease in cooling rate. Also, increased heat input generally results in a larger weld pool size and fused area.

Christensen (Ref. 14) developed a relationship based on Rosenthal's equations to correlate operating parameter (n) and cross-sectional areas of weld zone and the "recrystallized" portion of the base metal heat-affected zone where

$$\text{Operating parameter (n)} = \frac{qs}{4\pi K\alpha\left(t_f - t_0\right)} \qquad (7)$$

In Equation 7, q = net heat input (cal/s), K = thermal conductivity of plate, α = thermal diffusivity, t_f = melting temperature of plate, t_0 = initial temperature of plate, and s = welding speed, cm/s.

It is also reported both the fused weld zone and recrystallized HAZ areas increase as the operating parameter (n) increases for almost all materials.

From the equation, the HAZ and, therefore, the widths of the different zones of the HAZ increase steadily with the increase in heat input. The trends shown in Fig. 4 confirm the findings of Christensen (Ref. 14) and other researchers.

Direct Effect of Process Variables

The direct effect of process variables on the dimensions of different zones of the HAZ are shown in Figs. 5–8. The effects are presented in order of their influence on HAZ dimensions.

Direct Effect of Wire Feed Rate (F)

Figure 5 shows the effects of F on different HAZ parameters. From the figure, it is clear all dimensions of the different HAZ regions, namely, width of the HAZ, WI, GGZ, and GRZ, increase with the increase of F. These effects are due to the fact that as F increases, the heat-input value also increases more or less proportionately. But the increase in heat input level results in a decrease in cooling rate, as explained previously. Therefore, the width of GGZ, GRZ, and WI all increase with the increase in F.

Effect of Welding Speed (S)

Many researchers have found that next to current, welding speed is the main factor controlling heat input and the dimensions of the HAZ. Figure 6 shows the effects of S on HAZ parameters. From the figure, the following facts are evident: the value of WI, GGZ, GRZ, and HAZ all decrease with the increase in S. This is because heat input is inversely proportional to welding speed. As S increases, heat input decreases. Also, as per Christensen's (Ref. 14) empirical relationship

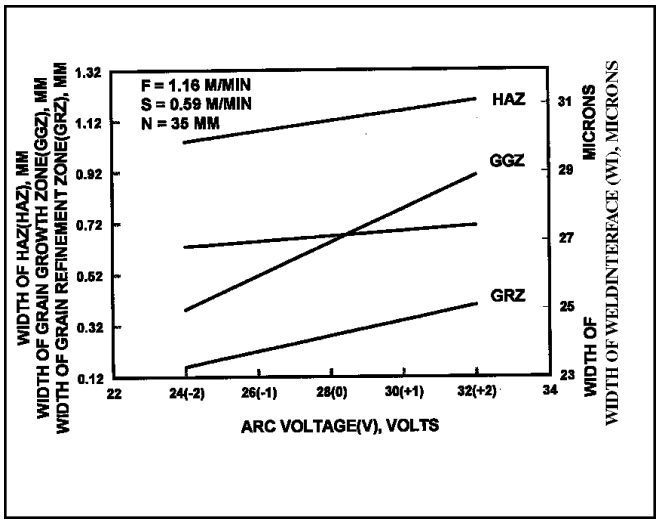

Fig. 7 — Direct effect of arc voltage on the width of the different HAZ regions.

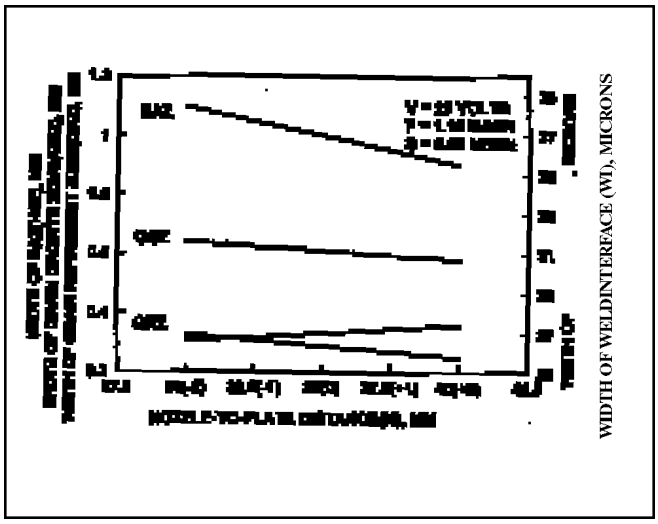

Fig. 8 — Direct effect of nozzle-to-plate distance on the width of the different HAZ regions.

between welding speed and HAZ dimensions, S has a negative effect on HAZ dimensions because of its influence on heat input. But, keeping heat input at a constant level, if S is increased, it will have a positive effect on most of the dimensions of the HAZ because faster travel speeds allow a greater portion of arc energy per unit length to be utilized in melting the base metal rather than just extending the magnitude of heating into the base metal beyond the boundary of the fused zone. In this investigation, heat input was not controlled. Therefore, S has a negative effect on heat input and on all the dimensions of the HAZ.

Table 5 — Comparison of Squared Multiple R Values and Standard Error of Estimates for Full and Reduced Mathematical Models

Sl. No. Reduced	Bead Parameters	R^2 Value (adjusted) Full models	Reduced models	Standard Error of Estimate Full models	Reduced models
1	Heat input	0.975	0.978	0.348	0.328
2	Width of HAZ	0.872	0.914	0.081	0.066
3	Width of weld interface	0.863	0.880	3.037	3.018
4	Width of grain growth zone	0.751	0.789	0.062	0.057
5	Width of grain refinement zone	0.893	0.990	0.039	0.036

Direct Effects of Arc Voltage

Many investigators (Refs. 1, 15) found voltage in a consumable electrode process has no significant effect on HAZ dimensions. In this investigation, it was found the effect of V is less than that of F on HAZ. Figure 7 shows the effect of V on the dimensions of different zones of the HAZ. From the figure, it is apparent WI, GRZ, and HAZ increase slightly with the increase in V; GGZ increases significantly with the increase in V. The reason for these effects is the slight increase in heat input (heat input increases by about 4 kJ/cm) with the increase in V from its lower limit (–2 level) to upper limit (+2 level). This slight increase in heat input reduces the cooling rate. Therefore, the dimensions of the different HAZ layers increase with the increase in V.

Effects of Nozzle-to-Plate Distance (N)

It is found N has a negligible effect on most HAZ dimensions within the range evaluated — Fig. 8. From this figure, it is clear WI increases slightly with the increase in N. It was also found GGZ, GRZ, and, therefore, HAZ decrease slightly with the increase in N. This slight decrease in HAZ (from 1.02 to 0.97 mm) might be due to the decrease in heat input from 10.2 to 9.5 kJ/cm when N is increased from the –2 to +2 level (as evident from the 23rd and 24th experimental runs shown in Table 2). As heat input has a positive effect on the HAZ, the slight decrease in heat input (by about 0.7 kJ/cm as N is increased from 30 to 40 mm) results in a slight decrease in the values of the GGZ, GRZ, and HAZ.

Interaction Effects of Process Variables

From the final mathematical models, it is noted the process variables have many interaction effects on the HAZ dimensions, but only a few select and important interaction effects are presented in graphical form for analysis. Interaction effects of the selected process variables on various HAZ dimensions are shown in Figs. 9–14.

Interaction Effects of Wire Feed Rate and Welding Speed on HAZ

Figure 9 shows the HAZ increases with the increase in F for all values of S, but the rate of increase in HAZ is steady and greater when S is at its lower limit (–2 level). This is because F has a positive effect, but S has a negative effect on HAZ, as discussed previously. HAZ is maximum (about 2.1 mm) when F and S are respectively at their upper (+2) and lower (–2) limits. HAZ is minimum (about 0.7 mm) when F and S are respectively at their lower and upper limits. The decrease in the rate of increase in the HAZ when S is increased indicates that at a lower value of S, the net effect on HAZ is the combined positive effect of F and S. But at higher values of S, the negative effect of S in decreasing HAZ is predomi-

Table 6 — Comparison of Actual and Predicted Values of HAZ Characteristics

	Process parameters in coded form				Predicted values of HAz characteristics				Actual values of bead characteristics				error %			
S. No.	V	F	S	N	HAZ mm	WI µm	GGZ mm	GRZ mm	HAz mm	WI µm	GGZ mm	GRZ mm	HAZ mm	WI µm	GGZ mm	GRZ mm
1	1.5	–0.5	–1.5	1.5	1.38	49.8	0.86	0.46	1.35	51	0.88	0.47	–2.2	2.4	2.3	2.17
2	–0.5	1.0	0.5	–0.5	1.15	33.7	0.68	0.36	1.12	32.9	0.70	0.36	–2.6	–2.4	2.9	00
3	1.2	–1.2	1.0	–1.2	1.02	29.1	0.55	0.25	1.05	30	0.54	0.26	2.9	3.1	–1.8	4.0
4	–1.5	1.5	–1.2	1.5	1.5	62.6	0.88	0.60	1.5	63.9	0.89	0.62	00	2.0	2.3	3.33
											Average Error		–0.48	1.28	1.43	2.4

$$\% \text{ Error} = \frac{\text{Actual value-Predicted value}}{\text{Predicted value}} \times 100$$

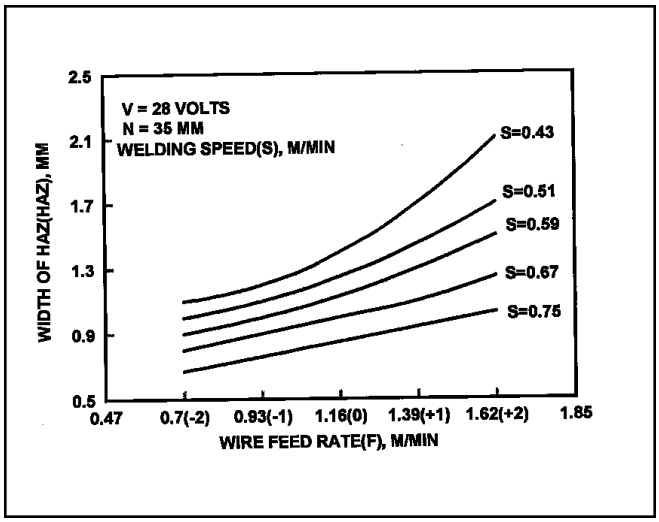

Fig. 9 — Interaction effect of wire feed rate and welding speed on HAZ width.

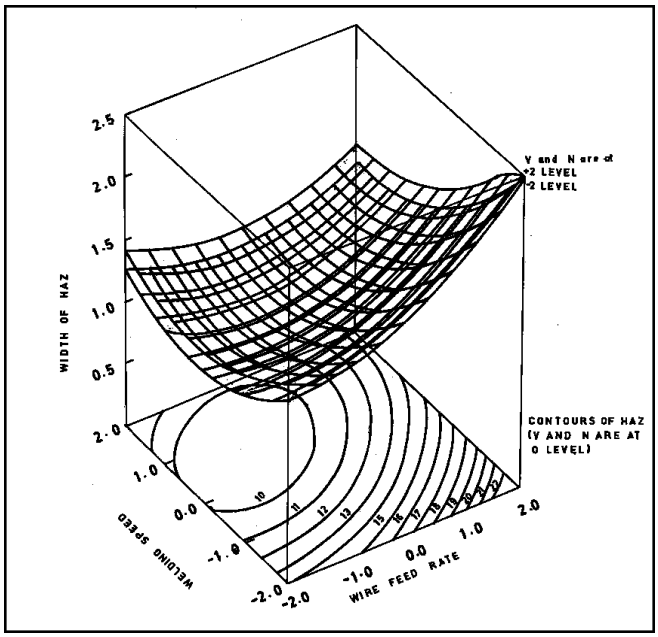

Fig. 10 — Response surface model for interaction effect of wire feed rate and welding speed on HAZ width.

nant over the positive effect of F on HAZ.

These effects are further explained with the help of a response surface plot, as shown in Fig. 10. From the contour surface, it is noted HAZ is maximum (about 2.2 mm) when F and S are respectively at their maximum (+2) and minimum (–2) limits, and the lowest value of HAZ (about 1.0 mm) is obtained when F and S are at their minimum and maximum limits, respectively. It is also observed that maximum value of the HAZ is obtained when both V and N are at their +2 limits and vice versa.

Interaction of Wire Feed Rate (F) and Welding Speed (S) on Width of Weld Interface (WI)

Figure 11 represents the interaction effect of F and S on the width of the weld interface. From the figure, it is clear WI increases with the increase in F for all values of S, but the rate of increase in WI gradually decreases with the increase in S. This is because F has a positive effect but S has a negative effect on heat input. Maximum WI value is obtained (about 72 mm) when F is at its upper limit (+2 level) with S at its lower limit (–2 level). Minimum WI value (about 22 mm) is obtained when F is at its lower limit (–2 level) with S at 0.67 m/min (+1 level). These effects show that at lower values of S, the combined effects of F and S are the net effect on WI, but at higher values of S, the negative effect of S in decreasing WI is found to be stronger than the positive effects of F.

This is also shown clearly by the response surface plot depicted in Fig. 12. It is evident from the contour plot that WI is maximum for all values of F and S when V and N are at their upper limits, and WI is minimum for all values of F and S when V and N are at their lower limits.

Interaction of F and S on Width of Grain Growth Zone (GGZ)

Figure 13 shows the interaction effects of F and S on GGZ are similar to that of F and S on WI. The reason for the increasing trend of GGZ with the increase in F is the positive effect of F. The gradual decrease in the increasing rate of GGZ with the increase in S is due to the negative effect of S. At lower values of S, heat input increases with the increase in F. As the heat input has a positive effect on GGZ, as explained previously, it increases with the increase in F. This shows the net effect is the combined effect of F and S on GGZ, but, at higher values of S, the negative effect of S is stronger than the positive effect of F on GGZ. Therefore, the increasing trend of GGZ decreases gradually as S is increased.

It is also evident from the contour plot shown in Fig. 14 that width of the GGZ is

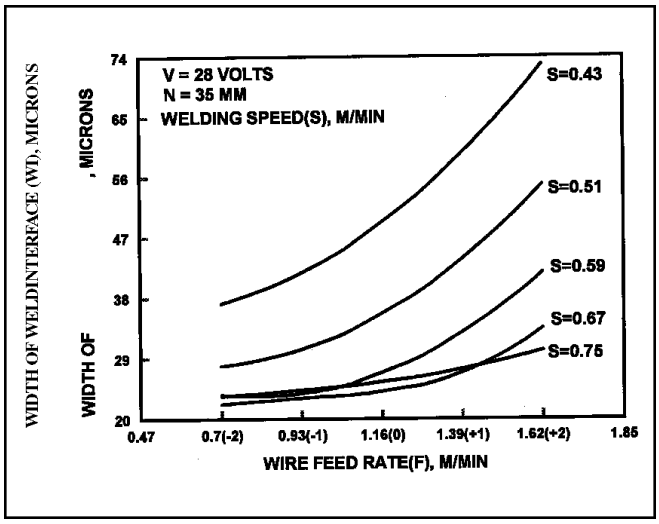

Fig. 11 — Interaction effect of wire feed rate and welding speed on width of the weld interface.

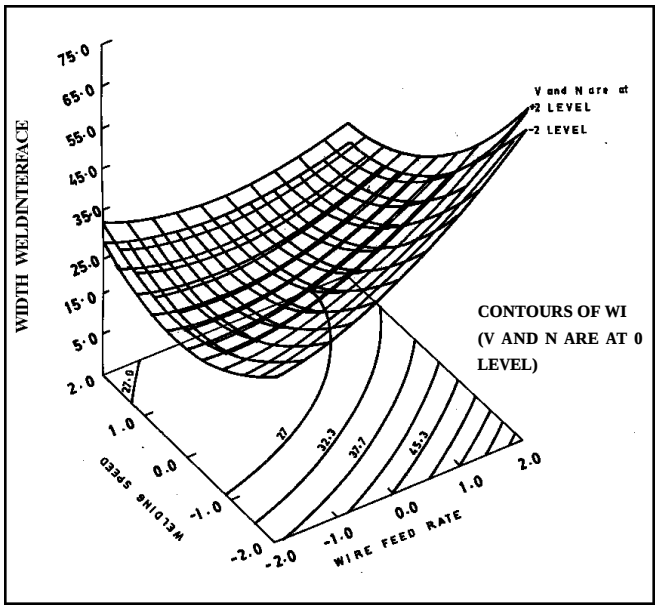

Fig. 12 — Response surface model for interaction effect of wire feed rate and welding speed on width of the weld interface.

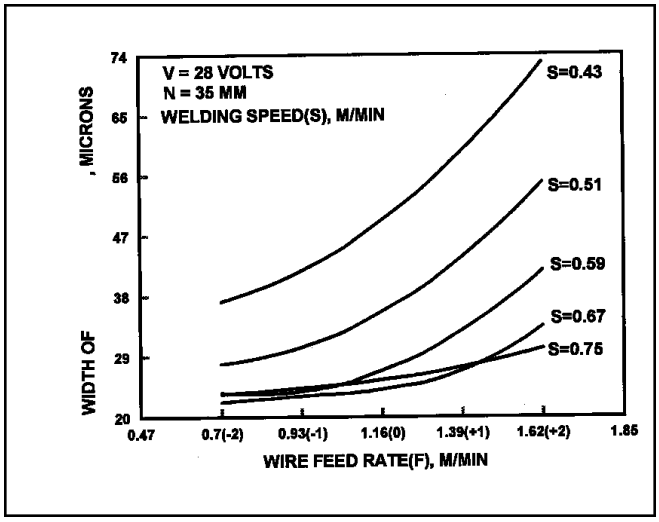

Fig. 13 — Interaction effect of wire feed rate and welding speed on width of grain growth zone.

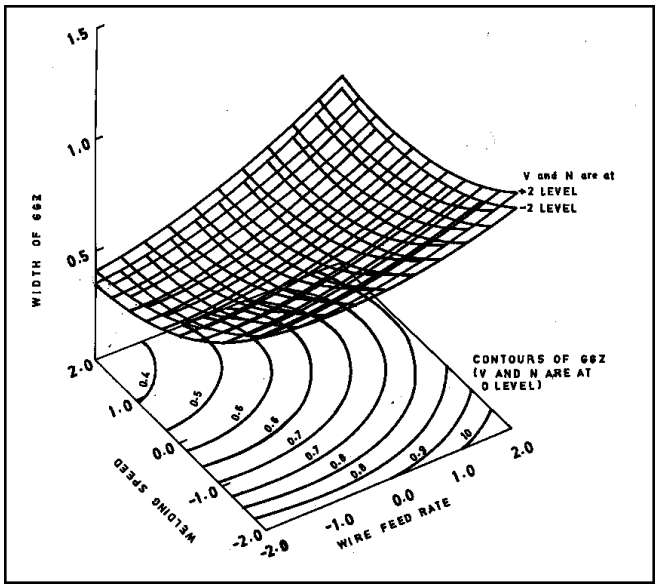

Fig. 14 — Response surface model for interaction effect of wire feed rate and welding speed on width of grain growth zone.

maximum when F and S are at the +2 and –2 levels, respectively. It is also evident from the plot the width of the GGZ surface is shifted below when V and N are changed from their +2 to –2 levels; therefore, the GGZ decreases for all values of F and S when V and N are lowered.

Conclusions

1) The second order quadratic mathematical models are useful for predicting and controling the dimensions of different regions of the HAZ of a weldment.

2) Validation of the models and comparison of the predicted and observed values of bead parameters revealed the models' average accuracy is about 97%.

3) Heat input — calculated using welding current, welding voltage, and welding speed — had a considerable positive effect on almost all HAZ dimensions.

4) Wire feed rate had a positive effect but welding speed had a negative effect on all HAZ dimensions.

5) Within the values evaluated, nozzle-to-plate distance had no considerable effect on most HAZ dimensions. The dimensions of the grain growth zone, grain refinement zone, and, therefore, the width of the heat-affected zone decreased slightly with the increase in nozzle-to-plate distance.

6) Out of the different process variables, wire feed rate and welding speed had a strong interaction effect on HAZ dimensions.

7) The increasing trend (rate) of the widths of the weld interface, grain growth zone, and HAZ with the increase in wire feed rate gradually decreased with the increase in welding speed. For instance,

maximum value of the HAZ width was 2.1 mm when F and S were, respectively, at their upper and lower limits, but the HAZ width was minimum (0.7 mm) when F and S were, respectively, at their lower and upper limits.

References

1. Linnert, G. E. 1994. Welding Metallurgy, vol. 1, 4th ed. Miami, Fla.: American Welding Society.

2. Lancaster, J. F. 1987. The Metallurgy of Welding, 4th ed. London, England: Allen and Unwin, pp. 168–170.

3. Patchett, B. M., et al. 1987. Control of microstructure and mechanical properties in SA and GMA weld metals. Proceedings of an International Symposium on Welding Metallurgy of Structural Steels, Colorado, pp. 189–199.

4. Adler, Y. P., Markov, E. V., and Granovsky, Y. V. 1975. The Design of Experiments to Find Optimal Conditions. Moscow, USSR: MIR Publishers.

5. Fisher, R. A. 1952. Statistical Methods for Research Workers, 12th ed. Edinburgh, Scotland: Oliver and Boyd.

6. Gupta, V. K., and Parmar, R. S. 1986. Fractional factorial techniques to predict dimensions of the weld bead in automatic submerged arc welding. Journal of Inst. of Engineers (India) 70: 67–71.

7. Box, G. E. P., et al. 1978. Statistics for Experimenters: An Introduction to Design Data Analysis and Model Building, 10th ed. New York, N.Y.: John Wiley and Sons.

8. Arya, S. K., and Parmar, R. S. 1986. Mathematical models for predicting angular distortion in CO_2 shielded flux cored arc welding. Proceedings of the International Conference on Joining of Metals (JOM–3), Helsingor, Denmark, pp. 240–245.

9. Murugan, N., and Parmar, R. S. 1994. Effects of MIG process parameters on the surfacing of stainless steel. Journal of Materials Processing Technology 41: 381–398.

10. Cochran, W. G., and Cox, G. M. 1963. Experimental Designs. India, Asia Publishing House.

11. Montagomery, D. C., and Peck, E. A. 1962. Introduction to Linear Regression Analysis. New York, N.Y.: John Wiley and Sons.

12. Davis, O. L. 1978. The Design and Analysis of Industrial Experiments. New York, N.Y.: Longman.

13. Wilkinson, L. 1990. SYSTAT: The System for Statistics. SYSTAT, Inc., Evanston, Ill.

14. Christensen, N. 1965. Distribution of temperature in arc welding. British Welding Journal, 12(2): 54–57.

15. Easterling, K. E. 1983. Introduction to the Physical Metallurgy of Welding. London, U.K.: Chapman and Hall.

Submerged Arc Welding of Steel A Review of Thermography used in Non-Destructive Testing (NDT) A Review on the Problem of Reheat Cracking in Nuclear Vessel Steels A Stress Intensity Factor Solution for Root Defects A Study of Arc and Friction Stir Welding of Two Al Alloys Containing a Low Level Scandium Addition A Study of Ceramic/Metal Bonding A Study of the. Butt Fusion (Hot Plate) Welding Process for Polyethylene Pipe A Survey of Joining Techniques for Plastics A Survey of Welding and Repairing of Nickel Superalloys for Gas Turbines A System for Integrated Off-Line Programming of Welding Robots A Theoretical Investigation into Stresses Caused by Die-Bonding and the Validity of 'Low Stress' Die-Bonding Attachments A Thermal Model for Transmission Laser Welding. Submerged Arc Welding Power Source. Three-phase squarewave AC/DC machine with phase-shifting capability with steps to refine arc. AC/DC squarewave provides excellent quality of penetration/bead profile and high performance in deposition rate with low heat input (increased mechanical properties and reduced distortion). PROCESSES â€¢ Submerged Arc (SAW) â€¢ Electroslag (ESW). CHARACTERISTICS â€¢ CC/CV â€¢ AC/DC variable squarewave â€¢ Requires three-phase power â€¢ Easy to integrate [20] Murugan, N., Gunaraj, V., Prediction of Heat-Affected Zone Characteristics in Submerged Arc Welding of Structural Steel Plates, Welding Research, January, (2002), 94. [21] Dutta, P., Weld Pool Dynamics during Submerged Arc Welding Process, North Bengal University Review (Science & Technology), 9. [1] (1997) 83. [22] Sreedhar, U., Krishnamurthy, C.V., Balasubramaniam, K., Raghupathy, V.D. and Ravishankar, S., Modeling and Simulation for Temperature Prediction in Welding Using Infrared Thermography, Proceedings of the National Seminar & Exhibition on Non-Destructive Evaluation, NDE 2009, December 10-12 (2009). [23] Goldak, J.A., Akhlaghi, M., Computational Welding Mechanics, Springer, p.31.